

Enhanced ultraviolet upconversion emission using nanocavities

A. Elhalawany,^{1,2} W. E. Hayenga,¹ S. He,³ S. Alhasan,¹ C. Lantigua,¹ N. J. J. Johnson,³ A. Almutairi,³ and M. Khajavikhan,^{1*}

¹CREOL, College of Optics and Photonics, University of Central Florida, Orlando, Florida 32816-2700, USA

²Department of Physics, University of Central Florida, Orlando, Florida 32816, USA

³Skaggs School of Pharmacy and Pharmaceutical Sciences, KACST-UCSD Center of Excellence in Nanomedicine, Laboratory of Bioresponsive Materials, University of California, 9500 Gilman Dr., 0600, PSB 2270, La Jolla, San Diego, USA

*Corresponding author: mercedeh@creol.ucf.edu

Abstract: We investigate the upconversion emission spectra of Tm^{3+} and Yb^{3+} codoped: β - NaYF_4 - NaYF_4 core-shell nanoparticles embedded in plasmonic nanocavities. The results confirm the role of nanocavities in maximizing the conversion efficiency from the NIR to UV.

OCIS codes: (190.7220) Upconversion; (310.6628); Subwavelength structures, nanostructures;

Photon upconversion (UC) is an anti-stokes process in which the sequential absorption of two or more photons leads to the emission of light at a shorter wavelength. Materials for which UC can take place often contain ions of d-block and f-block elements [1,2]. Significant progress has been made in synthesizing codoped UC nanocrystals in which one type of doping (sensitizer) absorbs the radiation and transfers it to another type of doping (activator). Furthermore, the quenching through surface defects and non-radiative recombination has been substantially subdued by appropriately shelling the upconverting nanocrystals [3]. Despite these advancements, the low luminescence efficiency still remains a limiting factor for UC systems. In applications where several upconverting nanoparticles can be encapsulated in sub-micron size cavities, photonics and quantum optics can provide appropriate tools to further customize their emission spectra and radiation patterns.

In this Letter, we investigate the upconversion emission spectra of Tm^{3+} and Yb^{3+} codoped: β - NaYF_4 - NaYF_4 core-shell nanoparticles encapsulated in plasmonic nanocavities. Figure 1a depicts the geometry of the system. The UC nanoparticles are embedded in a thin film of polymer host with a matching refractive index of $n=1.5$ to form a cylindrical rod with a radius of 150nm and a height of 200nm [4]. The nanocavities are then formed by patterning cylindrical rods which are shelled by aluminum tubes as shown in Fig. 1a on the polymer. For enhancing the emission at the UV band, aluminum is the most suitable plasmonic metal. The presence of the metallic nanocavity alters the NIR absorption characteristic of the nanoparticles. Figure 1b and c compare the NIR absorption in the absence and presence of the metal cavity. The simulations show that in the presence of

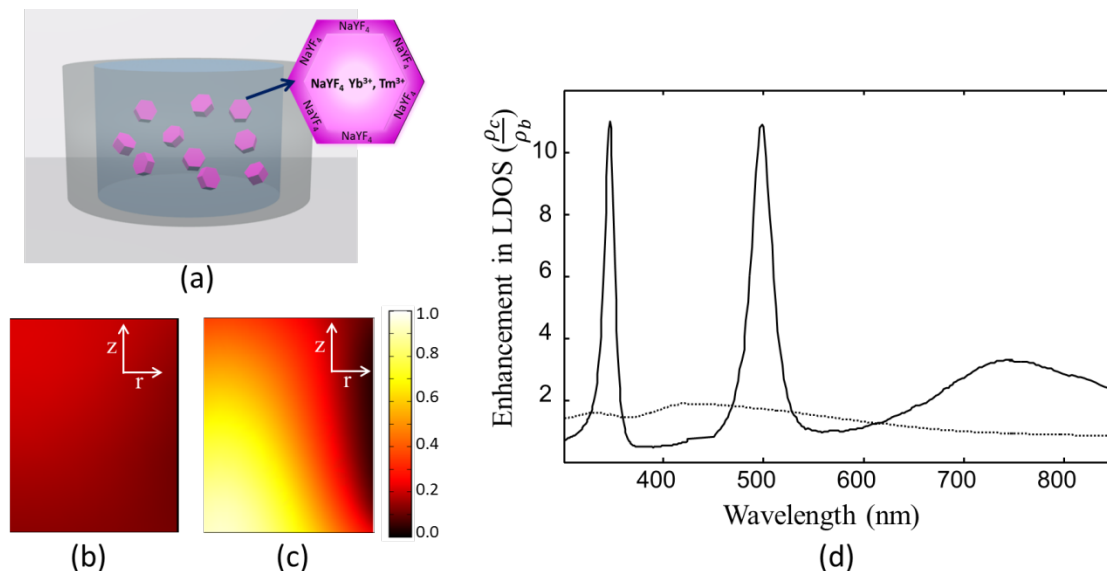


Figure 1 (a) Shows a schematic of the nanocavity containing upconversion β -phase NaYF_4 : Tm^{3+} Yb^{3+} - NaYF_4 core-shell nanoparticles. (b) Absorbed power density (watt per volume) at a wavelength of 980nm(NIR) in the polymer region by (b) UCNP-embedded in a bare cylindrical cavity. (c) The same structure when surrounded by an aluminum ring with thickness of 50 nm as depicted in Fig. 1a. (d) Enhancement factor of the LDOS for UCNP- embedded in a bare polymer cylindrical cavity (dashed line), and for the same structure when surrounded by an aluminum ring with a thickness of 50 nm (solid line). ρ_b and ρ_c are the local density of states in the bulk and in the cavity, respectively.

the nanocavity the absorption improves by a factor of three. In addition, the cavity alters the local density of states (LDOS). In particular, we identified more than a 12 time improvement in the LDOS at the UV spectral band as shown in fig. 1d.

Through these above two mechanisms, the nanoscale plasmonic cavity alters the dynamical response of the UC nanoparticles. This dynamic response is modeled by employing a set of rate equations adapted to these systems. The rate equations are given as follows,

$$\dot{n} = (M_{GSA} + M_{ESA} + M_{STE} + M_{MP} + M_{SPE})n + [ET], \quad (1)$$

where vector n represents populations of the involved energy bands which includes ${}^2F_{7/2}$ and ${}^2F_{5/2}$ levels of the activator (Yb^{3+}) ions, and 3H_6 , 3F_4 , 3H_5 , 3H_4 , 3F_2 & 3F_3 , 1G_4 , 1D_2 levels of the sensitizer (Tm^{3+}). The ground state absorption matrix (M_{GSA}) describes transitions between ${}^2F_{7/2}$ and ${}^2F_{5/2}$ of the activator ions, and similarly the excited state absorption matrix (M_{ESA}) dictates the transitions between the sensitizer's upper levels with energy separation corresponding to the excitation frequency. The stimulated emission (M_{STE}) matrix represents the rate of stimulated transitions at the excitation wavelength of 980 nm. The multi phonon matrix (M_{MP}) accounts for the non-radiative transitions between energy bands enabled by multiple phonon exchange between the host crystal and the sensitizer ions. Finally, the spontaneous emission matrix (M_{SPE}) represents the spontaneous radiative transitions between all energy bands involved. In addition to the above linear processes, a total of eight nonlinear processes are considered in our model that governs the energy transfer between the sensitizer and activator ions ($[ET]$). Half of these processes are UC energy transfers while the other half of them are cross relaxation mechanisms. The population of these higher levels is predominantly achieved through the succession of subsequent energy transfer steps from the activator ion, Yb^{3+} , to the sensitizer ion, Tm^{3+} .

Figure 2 shows the modified spectrum of the UC nanoparticles in the nanocavity. The numerical simulations based on the above rate equations shows more than 30-fold increase in conversion efficiency from near-infrared to the ultraviolet spectral band due to the engineering of the absorption and LDOS.

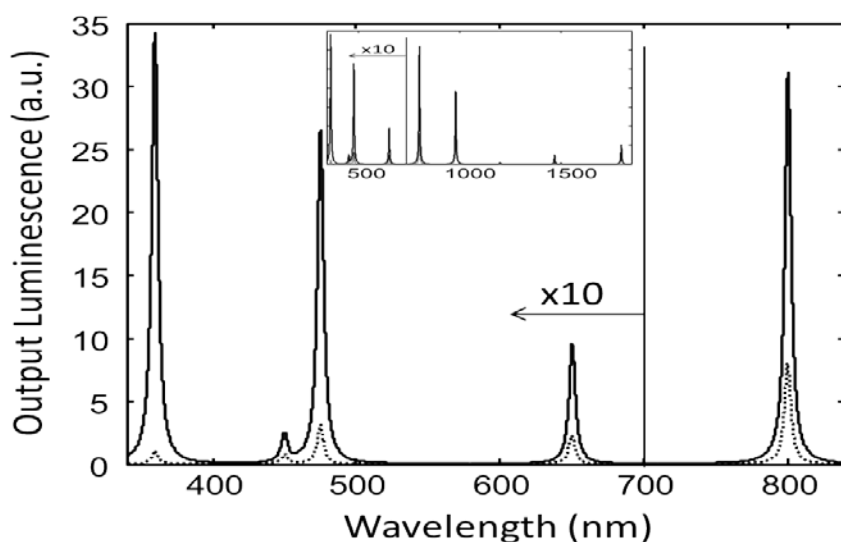


Figure 2 Spectrum of the $\text{NaYF}_4: \text{Tm}^{3+} \text{Yb}^{3+}$ UC nanoparticles. The dotted line represents the luminescence spectrum of UCNPs in a polymer rod, while the solid line depicts the luminescence spectrum of UCNPs in the aluminum tubed nanocavity. The inset shows the full spectrum (340-1840 nm). Below 700 nm, the emission is magnified by an order of magnitude to facilitate visual comparisons.

To experimentally verify our results, the UC nanoparticles are assimilated in a HSQ polymer matrix. Nano-patterning is performed by electron beam lithography. The aluminum is deposited using electron beam evaporation. The fabricated structures will be characterized to investigate the emission properties of individual UC capsules or a cluster of them. In order to distinguish effects arising from plasmonic patterning, samples with no metallic tubes will also be examined.

References

- [1] N. Bloembergen, "Solid state infrared quantum counters." *Physical Review Letters* **2**, 84 (1959)
- [2] F. Auzel, "Upconversion and anti-stokes processes with f and d ions in solids." *Chemical reviews* **104**, 139-174 (2004).
- [3] F. Wang, D. Banerjee, Y. Liu, X. Chen, and X. Liu, "Upconversion nanoparticles in biological labeling, imaging, and therapy." *Analyst* **135**, 1839-1854 (2010).
- [4] A. Shalav, B. S. Richards, and M. A. Green, "Luminescent layers for enhanced silicon solar cell performance: Up-conversion." *Solar Energy Materials and Solar Cells* **91**, 829-842 (2007).